COPRIME DFT FILTER BANK DESIGN: THEORETICAL BOUNDS AND GUARANTEES

Chun-Lin Liu[1] *and P. P. Vaidyanathan*[2]

Dept. of Electrical Engineering, 136-93
California Institute of Technology, Pasadena, CA 91125, USA
E-mail: cl.liu@caltech.edu[1] and ppvnath@systems.caltech.edu[2]

ABSTRACT

Coprime DFT filter banks (coprime DFTFB) achieve the effect of an MN-DFTFB by using two DFTFBs of size only M and N, where M and N are coprime integers. However, coprime DFTFBs need to be designed properly, to avoid unwanted bumps in stopbands or unsatisfactory total spectrum coverage, quantified by overall amplitude responses. In this paper, a detailed theoretical analysis will be made on the tradeoffs between bumps and overall amplitude responses. It will be shown that the bump level at the center frequency f_b of a bump, is approximately one-fourth of the overall amplitude response at f_b. Then, a novel design will be introduced based on an optimization problem pertaining to overall amplitude responses. The original problem is relaxed to a computationally tractable optimization program, which can be solved with alternating minimization algorithms. It is verified with simulations that the new designs cover the spectrum completely.

Index Terms— Coprime arrays, coprime DFT filter banks, spectrum sensing.

1. INTRODUCTION

Recently, coprime arrays and coprime DFT filter banks (coprime DFTFBs) [1] have received attention in array processing, direction-of-arrival estimation [2], system stabilization [3], and power spectrum estimation [4]. Provided with two coprime integers M and N, the degrees of freedom (DOFs) are enhanced to $O(MN)$ with only $O(M + N)$ sensors or samples. Thus it is possible to identify more sources than the number of sensors [2]. Another advantage of coprime arrays is its simplicity, compared to other increased DOF arrays such as minimum redundancy arrays (MRAs) [5]. Coprime arrays are defined based on two coprime integers M and N, leading to two uniform linear arrays (ULAs). On the other hand, MRAs do not own a closed-form array geometry.

The coprime DFTFB design was first considered in [1]. Three different designs were discussed: 1) uniform weightings, 2) optimal weightings using the Remez algorithm, and 3) extended elements using optimal weightings. However, these designs only showed that practical filters could be achieved by higher filter orders and the Remez algorithm. There were no design guidelines on the mainlobe width, sidelobe level, and other filter specifications.

Adhikari *et al.* considered an extended coprime array with uniform weighting in [6]. The optimal choice of M and N were first found and then an additional parameter a was introduced to limit the peak side lobe level, which corresponds to bumps in this paper.

However, the optimal weighting was not included in [6] and the filter specifications could not be arbitrarily designed.

The design issues of coprime DFTFBs were addressed in [7], which is fundamental to beamforming and power spectrum estimation applications. Inspired by interpolated FIR (IFIR) concepts [8–10], a systematic design procedure was proposed based on the specifications such as passband/stopband ripples and bandedges. Also, there are bumps due to overlap of filter images. The unwanted bumps in coprime DFTFBs were eliminated by an appropriate choice of bandedges [7]. However, this design leads to dips in the overall amplitude response of the filter bank. Sources around these dips might be rejected down to the noise floor, causing a blind region on the parameter space.

In this paper, we establish the exact theoretical tradeoffs between overall amplitude responses and bumps. Then we consider another approach to coprime DFTFBs, based on the spectrum coverage concept. This criterion is formulated as a nonconvex optimization and further relaxed to another problem, that can be solved alternatively with convex optimization solvers.

This paper is organized as follows. Basics of coprime DFTFB and its design procedures are described in Section 2. Bumps are analyzed in detail in Section 3 and the optimization problem is proposed in Section 4. Numerical examples on actual filter design are given in Section 5 before concluding this paper in Section 6.

2. REVIEW OF COPRIME DFTFB DESIGN

For coprime integers M and N, define two real coefficient lowpass FIR filters

$$G(z) = \sum_{n=0}^{N_g} g(n)z^{-n}, \qquad H(z) = \sum_{n=0}^{N_h} h(n)z^{-n}.$$

The coprime DFTFB is a set of MN filters defined as follows

$$F_{\ell k}(z) = G\left(z^M W_N^\ell\right) H\left(z^N W_M^k\right), \qquad (1)$$

where $0 \leq \ell \leq N - 1$, $0 \leq k \leq M - 1$, and $W_N = e^{-j2\pi/N}$. In [1], it was shown that if $G(z)$ and $H(z)$ are ideal lowpass filters with bandwidth $1/N$ and $1/M$, respectively, then $F_{\ell k}(z)$ are a set of MN filters with bandwidth $1/(MN)$ covering the whole spectrum. These properties lead to an efficient implementation of coprime DFTFBs. Firstly, $G\left(z^M W_N^\ell\right)$ and $H\left(z^N W_M^k\right)$ admit a polyphase implementation, which has low cost compared to an MN-band filter bank. Secondly, (1) can be realized by statistical averaging over the cross products of outputs of $\left\{G\left(z^M W_N^\ell\right)\right\}$ and $\left\{H\left(z^N W_M^k\right)\right\}$. Hence, a more dense set of MN bands is achieved with the cost of approximately two smaller size DFTFBs.
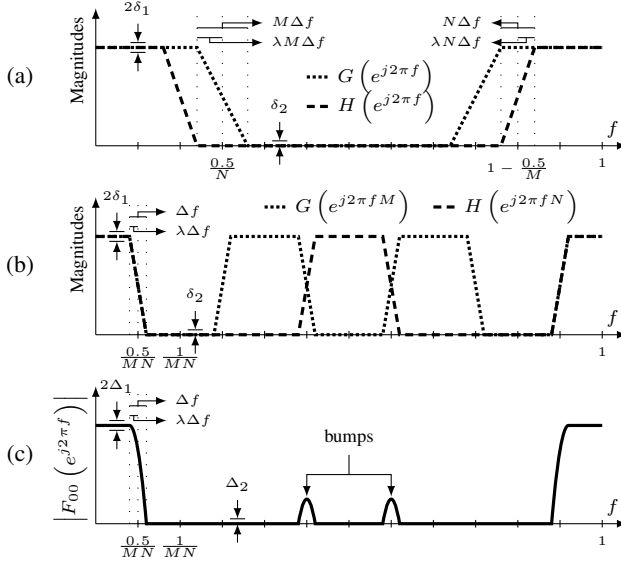
Fig. 1. An illustration of coprime DFTFB for $M = 3$ and $N = 2$. (a) Prototype filters $G\left(e^{j2\pi f}\right)$ and $H\left(e^{j2\pi f}\right)$. (b) Magnitude responses of sparse coefficient filters $G\left(e^{j2\pi fM}\right)$ and $H\left(e^{j2\pi fN}\right)$. (c) The first filter ($F_{00}\left(e^{j2\pi f}\right) = G\left(e^{j2\pi fM}\right)H\left(e^{j2\pi fN}\right)$) in coprime DFTFB.

Coprime DFTFB designs compute impulse responses $g(n)$ and $h(n)$ based on specifications on filter banks. Fig. 1 illustrates a typical coprime DFTFB design in [7]. The coprime integers M, N, passband/stopband ripples Δ_1 and Δ_2 and the filter orders N_g as well as N_h are given. The parameter λ offers tradeoffs between the bumps and the passband width. Different closed-form functions were utilized to approximate the transition bands and yield good choices of $\hat{\lambda}$. The details of this design method can be found in [7].

3. BUMP ANALYSIS IN COPRIME DFTFBS

In this section we will prove a number of theorems related to coprime DFTFB responses. As seen from Fig. 1(c), bumps arise because of overlap of transition bands of $G\left(e^{j2\pi fM}\right)$ and $H\left(e^{j2\pi fN}\right)$. It will be proved that the number of bumps in $F_{\ell k}\left(e^{j2\pi f}\right)$ is exactly two and the location of bumps can be uniquely determined in terms of M and N. The overall amplitude response is defined as

$$A\left(e^{j2\pi f}\right) = \sum_{\ell=0}^{N-1}\sum_{k=0}^{M-1}\left|F_{\ell k}\left(e^{j2\pi f}\right)\right|, \tag{2}$$

which is important because it represents the spectrum coverage of coprime DFTFB. If $A\left(e^{j2\pi f}\right)$ exhibits dips at certain frequencies, the detection performance might degrade greatly. Later on, we will prove that there are tradeoffs between bump levels and $A\left(e^{j2\pi f}\right)$. The bump level at the center frequency f_b of a bump is approximately $\frac{1}{4}A\left(e^{j2\pi f_b}\right)$. It will be assumed that M and N are greater than 1 in the following context so that it does not reduce to the special case of IFIR designs.

Definition 1. *A bump in coprime DFTFB results from overlapping between the finite transition bands of the sparse coefficient filters $G\left(e^{j2\pi fM}\right)$ and $H\left(e^{j2\pi fN}\right)$.*

As an example, the bumps in Fig. 1 occurs at $f = 2.5/(MN)$ and $f = 3.5/(MN)$.

Lemma 1. *For any $0 \le \ell \le N-1, 0 \le k \le M-1$, there exists $f_0 \in [0,1)$ such that $\left|F_{\ell k}\left(e^{j2\pi f}\right)\right| = \left|F_{00}\left(e^{j2\pi(f-f_0)}\right)\right|$.*

Proof. Starting with the left-hand side of the equation gives

$$\left|F_{\ell k}\left(e^{j2\pi f}\right)\right| = \left|G\left(e^{j2\pi fM}e^{-j2\pi\ell/N}\right)H\left(e^{j2\pi fN}e^{-j2\pi k/M}\right)\right|$$
$$= \left|G\left(e^{j2\pi fM}e^{-j2\pi\ell/N}e^{-j2\pi\ell'}\right)H\left(e^{j2\pi fN}e^{-j2\pi k/M}e^{-j2\pi k'}\right)\right|$$
$$= \left|G\left(e^{j2\pi M\left(f-\frac{\ell}{MN}-\frac{\ell'}{M}\right)}\right)H\left(e^{j2\pi N\left(f-\frac{k}{MN}-\frac{k'}{N}\right)}\right)\right|,$$

where ℓ' and k' are integers. Setting the amount of shift in f to be f_0 results in the following equation,

$$MNf_0 = N\ell' + \ell = Mk' + k.$$

Given ℓ and k, MNf_0 can be determined by the Chinese remainder theorem (CRT) [11]. This completes the proof. $\square$

Theorem 1. $F_{\ell k}\left(e^{j2\pi f}\right)$ *contains exactly two bumps for any $0 \le \ell \le N-1, 0 \le k \le M-1$.*

Proof. The first filter of coprime DFTFBs is $F_{00}\left(e^{j2\pi f}\right) = G\left(e^{j2\pi fM}\right)H\left(e^{j2\pi fN}\right)$. The passbands of $G\left(e^{j2\pi fM}\right)$ are centered at frequencies $f = m/M, m \in \{0,1,\ldots,M-1\}$. The same argument for $H\left(e^{j2\pi fN}\right)$ gives the center frequencies $f = n/N, n \in \{0,1,\ldots,N-1\}$. Bumps occur when the transition bands of $G\left(e^{j2\pi fM}\right)$ and $H\left(e^{j2\pi fN}\right)$ overlap, implying $n/N - m/M = \pm 1/(MN)$ or

$$Mn - Nm = \pm 1. \tag{3}$$

Then we need to prove the existence and the uniqueness of the solution to (3):

(Existence): Euclid's theorem [11] implies that there exists integer solutions to (3). Assuming (m_0, n_0) is a solution to (3), we can uniquely rewrite it as

$$m_0 = m_0' + pM, \qquad n_0 = n_0' + qN. \tag{4}$$

where $m_0' \in \{0,1,\ldots,M-1\}, n_0' \in \{0,1,\ldots,N-1\}$, and p, q are integers. Putting (4) into (3) yields

$$\left(Mn_0' - Nm_0'\right) + (q-p)MN = \pm 1. \tag{5}$$

Based on the domain of (m_0', n_0'), the first term is limited to $Mn_0' - Nm_0' \in \{-MN + N, \ldots, MN - M\}$. The only choice matching the left-hand side with the right-hand side of (5) is $p = q$ and $Mn_0' - Nm_0' = \pm 1$.

(Uniqueness): Assume there exist two distinct solutions (m, n) and (m', n') to (3). Rearranging the equations gives

$$M\left(n - n'\right) = N\left(m - m'\right).$$

Then $n - n'$ is divisible by N. Nevertheless, $n - n' \in \{-(N-1), \ldots, -1, 1, \ldots, N-1\}$, which makes it impossible to be divisible by N. Therefore, the solutions to (3) is unique.

We write the unique solutions (m_+, n_+) and (m_-, n_-) corresponding to ± 1 in (3), respectively. Each set of solution uniquely determines a bump in $F_{00}\left(e^{j2\pi f}\right)$, meaning $F_{00}\left(e^{j2\pi f}\right)$ contains exactly two bumps. Then the proof is completed using Lemma 1. $\square$

Theorem 2. *The two bumps of $F_{00}\left(e^{j2\pi f}\right)$ are located around $f = u/(2MN)$ and $f = v/(2MN)$ with*

$$u = 2Mn_+ - 1 = 2Nm_+ + 1 \notin \{-1, 0, 1\},$$
$$v = 2Mn_- + 1 = 2Nm_- - 1 \notin \{-1, 0, 1\},$$

where $m_\pm \in \{0, 1, \ldots, M-1\}$, $n_\pm \in \{0, 1, \ldots, N-1\}$, and $Mn_\pm - Nm_\pm = \pm 1$. Also, the amplitude response of $F_{00}\left(e^{j2\pi f}\right)$ satisfies

$$\left|F_{00}\left(e^{\frac{j\pi}{MN}}\right)\right| = \left|F_{00}\left(e^{\frac{-j\pi}{MN}}\right)\right| = \left|F_{00}\left(e^{\frac{j\pi u}{MN}}\right)\right| = \left|F_{00}\left(e^{\frac{j\pi v}{MN}}\right)\right|.$$

Proof. Following the proof of Theorem 1, passbands of $G\left(e^{j2\pi fM}\right)$ and $H\left(e^{j2\pi fN}\right)$ are centered around $f = m_\pm/M$ and $f = n_\pm/N$, respectively. The two bumps locate around $f = (m_\pm/M + n_\pm/N)/2$. Combining (3) with bump locations yields

$$\frac{Mn_\pm + Nm_\pm}{2MN} = \frac{2Mn_\pm \mp 1}{2MN} = \frac{2Nm_\pm \pm 1}{2MN}.$$

Then it will be proved that $u, v \notin \{-1, 0, 1\}$. If $u = -1$, we obtain $n_+ = 0$ and $Nm_+ = -1$, according to (3). There does not exist such solution to m_+. For $u = 0$, we have $2Mn_+ = 1$ but n_+ is an integer, which is not possible. $u = 1$ implies $m_+ = 0$ and $Mn_+ = 1$. Similar argument holds for v.

The first equations between magnitude responses of $F_{00}\left(e^{j2\pi f}\right)$ is trivial since $F_{00}\left(e^{j2\pi f}\right)$ is a real coefficient FIR filter. The second equality is proved as follows:

$$\left|F_{00}\left(e^{j\frac{\pi u}{MN}}\right)\right| = \left|G\left(e^{j\frac{\pi u}{N}}\right)\right|\left|H\left(e^{j\frac{\pi u}{M}}\right)\right|$$
$$= \left|G\left(e^{j2\pi\left(m_+ + \frac{1}{2N}\right)}\right)\right|\left|H\left(e^{j2\pi\left(n_+ - \frac{1}{2M}\right)}\right)\right|$$
$$= \left|F_{00}\left(e^{j\frac{\pi}{MN}}\right)\right|.$$

$\left|F_{00}\left(e^{j\frac{\pi v}{MN}}\right)\right|$ follows the same derivation. $\square$

Theorem 3. *Assume the stopband ripples for $G\left(e^{j2\pi f}\right)$ and $H\left(e^{j2\pi f}\right)$ are ϵ_1 and ϵ_2, respectively. The bump level in coprime DFTFB is bounded by*

$$L \le \left|F_{00}\left(e^{\frac{j\pi p}{MN}}\right)\right| \le U,$$

where

$$L = \frac{1}{4}\left(A\left(e^{\frac{j\pi p}{MN}}\right) - \epsilon\right), \qquad U = \frac{1}{4}A\left(e^{\frac{j\pi p}{MN}}\right),$$
$$\epsilon = 2\left(N-2\right)\epsilon_1 + 2\left(M-2\right)\epsilon_2 + \left(M-2\right)\left(N-2\right)\epsilon_1\epsilon_2,$$

$p \in \{\pm 1, u, v\}$. Here u and v are defined in Theorem 2.

Proof. Putting $f = 1/(2MN)$ into (2) results in

$$A(e^{j\frac{\pi}{MN}}) = \sum_{\ell=0}^{N-1}\sum_{k=0}^{M-1}\left|G\left(e^{j\frac{M\pi}{MN}}W_N^\ell\right)H\left(e^{j\frac{N\pi}{MN}}W_M^k\right)\right|$$

$$= \left(\left|G\left(e^{j\frac{\pi}{N}}\right)\right| + \left|G\left(e^{-j\frac{\pi}{N}}\right)\right| + \sum_{\ell=2}^{N-1}\left|G\left(e^{j\left(\frac{\pi}{N} - \frac{2\pi\ell}{N}\right)}\right)\right|\right)$$

$$\times \left(\left|H\left(e^{j\frac{\pi}{M}}\right)\right| + \left|H\left(e^{-j\frac{\pi}{M}}\right)\right| + \sum_{k=2}^{M-1}\left|H\left(e^{j\left(\frac{\pi}{M} - \frac{2\pi k}{M}\right)}\right)\right|\right).$$

(6)

All these terms can be ordered as

$$0 \le \left|G\left(e^{j\left(\frac{\pi}{N} - \frac{2\pi\ell}{N}\right)}\right)\right| \le \epsilon_1 \le \left|G\left(e^{j\frac{\pi}{N}}\right)\right| \le 1, \qquad (7)$$

$$0 \le \left|H\left(e^{j\left(\frac{\pi}{M} - \frac{2\pi k}{M}\right)}\right)\right| \le \epsilon_2 \le \left|H\left(e^{j\frac{\pi}{M}}\right)\right| \le 1, \qquad (8)$$

for $\ell \in \{2, 3, \ldots, N-1\}$ and $k \in \{2, 3, \ldots, M-1\}$. From (6) - (8), and $A\left(e^{j2\pi f}\right) = A\left(e^{j2\pi\left(f + \frac{1}{MN}\right)}\right)$, Theorem 3 is proved. $\square$

Theorem 3 explains tradeoffs between bump levels and overall amplitude responses. The lower bound implies bumps are at least of the order of $A(e^{j\pi/(MN)})/4$ since the stopband ripples ϵ_1 and ϵ_2 are usually much smaller compared to $A(e^{j\pi/(MN)})$. In other words, it is impossible to eliminate a bump at the center frequency f_b of a bump while keeping $A\left(e^{j2\pi f_b}\right)$ close to 1. In [7], the simulations showed unwanted dips in $A\left(e^{j2\pi f}\right)$ because eliminating bumps was the main design goal.

4. COPRIME DFTFB DESIGN BASED ON ALTERNATING MINIMIZATION

In this section, a new design is proposed. This design procedure is preferred in applications where the spectrum coverage is more important than bumps. We will reformulate coprime DFTFB design as an optimization problem and solve its relaxed problem using convex solvers.

The cost function is composed of three factors in filters, summarized as follows

1. $\left|F_{00}\left(e^{j2\pi f}\right)\right|$ is close to unity in the passband.

2. $\left|F_{00}\left(e^{j2\pi f}\right)\right|$ is close to zero in the stopband.

3. Overall amplitude responses $A\left(e^{j2\pi f}\right)$ is close to unity at all frequencies.

The final cost function is a linear combination of these three factors. Assume that w_1, w_2, w_3 represent the weighting factor between them with $w_1 + w_2 + w_3 = 1, w_1, w_2, w_3 \ge 0$. Our optimization problem becomes

$$\min_{g(n),h(n)} \quad w_1 \left\|\left|F_{00}\left(e^{j2\pi f}\right)\right|_{f\in[0,\frac{1}{2MN})\cup\left(1-\frac{1}{2MN},1\right)} - 1\right\|_p$$

$$+ w_2 \left\|\left|F_{00}\left(e^{j2\pi f}\right)\right|_{f\in\left[\frac{1}{2MN},1-\frac{1}{2MN}\right]}\right\|_p$$

$$+ w_3 \left\|A\left(e^{j2\pi f}\right) - 1\right\|_p, \qquad (9)$$

where f is defined over a fine grid over $[0, 1)$. $\|\cdot\|_p$ denotes p-norm of a vector, where $F_{00}\left(e^{j2\pi f}\right)$ and $A\left(e^{j2\pi f}\right)$ are modelled as vectors over the frequency grid. However, (9) is not a convex program since the absolute values need to be taken entrywise.

Eq. (9) can be relaxed into a more tractable optimization program. Assuming $g(n)$ and $h(n)$ are type-I linear phase FIR filters, we obtain $\left|G\left(e^{j2\pi fM}\right)\right| = |G_1(f)|$ and $\left|H\left(e^{j2\pi fN}\right)\right| = |H_1(f)|$, where $G_1(f) = \sum_n a_n \cos\left(2\pi fMn\right)$ and $H_1(f) = \sum_n b_n \cos\left(2\pi fNn\right)$ for some real-valued $\{a_n\}$ and $\{b_n\}$ [10]. $G_1(f)$ might take negative values, but they happen only in stopbands and are much smaller than passband responses. Therefore, $\left|G\left(e^{j2\pi fM}\right)\right| \approx G_1(f)$, $\left|H\left(e^{j2\pi fN}\right)\right| \approx H_1(f)$, and (9) becomes

$$\min_{\mathbf{a},\mathbf{b}} \quad w_1 \left\|\mathbf{J}_p \times \left[(\mathbf{C}_M\mathbf{a}) \odot (\mathbf{C}_N\mathbf{b}) - \mathbf{1}\right]\right\|_p$$

$$+ w_2 \left\|\mathbf{J}_s \times \left[(\mathbf{C}_M\mathbf{a}) \odot (\mathbf{C}_N\mathbf{b})\right]\right\|_p$$

$$+ w_3 \left\|\mathbf{P} \times \left[(\mathbf{C}_M\mathbf{a}) \odot (\mathbf{C}_N\mathbf{b})\right] - \mathbf{1}\right\|_p, \qquad (10)$$

where "⊙" indicates the Hadamard product, $\mathbf{a}$ and $\mathbf{b}$ relate $g(n)$ and $h(n)$ as

$$\mathbf{a} = \begin{bmatrix} g\left(N_g/2\right) & 2g\left(N_g/2 - 1\right) & \ldots & 2g\left(0\right) \end{bmatrix}^T,$$
$$\mathbf{b} = \begin{bmatrix} h\left(N_h/2\right) & 2h\left(N_h/2 - 1\right) & \ldots & 2h\left(0\right) \end{bmatrix}^T.$$

Assume that $\mathbf{f} \in \mathbb{R}^{N_{\text{pt}}}$ is a column vector taking N_{pt} uniform samples over $[0, 1)$, where N_{pt} is a multiple of $2MN$. Let $\mathbf{C}_M \in \mathbb{R}^{N_{\text{pt}} \times \left(N_g/2+1\right)}$ and $\mathbf{C}_N \in \mathbb{R}^{N_{\text{pt}} \times \left(N_h/2+1\right)}$ be defined such that $[\mathbf{C}_M]_{i,j} = \cos\left(2\pi M A_{i,j}\right)$ and $[\mathbf{C}_N]_{i,j} = \cos\left(2\pi N B_{i,j}\right)$ where $\mathbf{A} = \mathbf{f}\mathbf{v}_1$, $\mathbf{B} = \mathbf{f}\mathbf{v}_2$, and

$$\mathbf{v}_1 = \begin{bmatrix} 0 & 1 & \ldots & N_g/2 \end{bmatrix}, \quad \mathbf{v}_2 = \begin{bmatrix} 0 & 1 & \ldots & N_h/2 \end{bmatrix}.$$

$\mathbf{J}_p$ and $\mathbf{J}_s$ select the passband and the stopband responses, respectively. They are defined as

$$\mathbf{J}_p = \begin{bmatrix} \mathbf{I}_{\frac{N_{\text{pt}}}{2MN}} & \mathbf{O}_{\frac{N_{\text{pt}}}{2MN} \times \left(N_{\text{pt}} - \frac{N_{\text{pt}}}{MN}\right)} & \mathbf{O}_{\frac{N_{\text{pt}}}{2MN}} \\ \mathbf{O}_{\frac{N_{\text{pt}}}{2MN}} & \mathbf{O}_{\frac{N_{\text{pt}}}{2MN} \times \left(N_{\text{pt}} - \frac{N_{\text{pt}}}{MN}\right)} & \mathbf{I}_{\frac{N_{\text{pt}}}{2MN}} \end{bmatrix},$$

$$\mathbf{J}_s = \begin{bmatrix} \mathbf{O}_{\left(N_{\text{pt}} - \frac{N_{\text{pt}}}{MN}\right) \times \frac{N_{\text{pt}}}{2MN}} & \mathbf{I}_{N_{\text{pt}} - \frac{N_{\text{pt}}}{MN}} & \mathbf{O}_{\left(N_{\text{pt}} - \frac{N_{\text{pt}}}{MN}\right) \times \frac{N_{\text{pt}}}{2MN}} \end{bmatrix},$$

where $\mathbf{I}$ and $\mathbf{O}$ represent identity matrices and zero matrices of the described size in (10). $\mathbf{P}$ is a right-circulant matrix with the top row

$$[\underbrace{\overbrace{1, 0, \ldots, 0}^{\frac{N_{\text{pt}}}{2MN}}, \overbrace{1, 0, \ldots}^{\frac{N_{\text{pt}}}{2MN}}, 0, \ldots, \overbrace{1, 0, \ldots, 0}^{\frac{N_{\text{pt}}}{2MN}}}_{N_{\text{pt}}}].$$

The column vector $\mathbf{1}$ consists of all 1's in its entries.

Even though (10) is not a convex program, it can be solved via alternating minimization [12, 13], i.e. fix one variable and solve for the other and alternate until the stopping criteria are met. In each iteration, a convex optimization problem involving p-norms is solved.

A good initial guess is essential for alternating minimization. In our designs, designs in [7] serve as good initial points for $\mathbf{a}$ and $\mathbf{b}$.

5. NUMERICAL RESULTS

In this section, we consider the three design examples

Design 1: The example of [7], where $M = 8$, $N = 5$, $N_g = 100$, $N_h = 160$, $\Delta_1 = 0.01$, $\Delta_2 = 0.001$, and $\lambda = \hat{\lambda}_Q = 0.86926$.

Design 2: $M = 8$, $N = 5$, $N_g = 100$, $N_h = 160$. Solve (10) by alternating minimization, where Design 1 above is set as the initial point. We choose $N_{\text{pt}} = 2560$, $w_1 = w_2 = w_3 = 1/3$ and $p = 1$.

Design 3: The same as Design 2 except $p = 2$.

These three designs are plotted in Fig. 2. It is observed from Fig. 2(a) that Design 1 owns the smallest passband width. The bumps are visualized in Fig. 2(b), where Design 2 and 3 have bumps around $f = 0.3875$. Overall amplitude responses show tradeoffs stated in Theorem 3. A very wide dip is present in Design 1, but in Design 2 and 3, $A\left(e^{j2\pi f}\right)$ oscillate around unity. It can be concluded from Fig. 2 that Design 2 works even better than Design 3 in terms of achieving smaller perturbations in $A\left(e^{j2\pi f}\right)$. Therefore, if the spectrum coverage is of the main concern in our applications, Design 2 is the best design among all three designs.
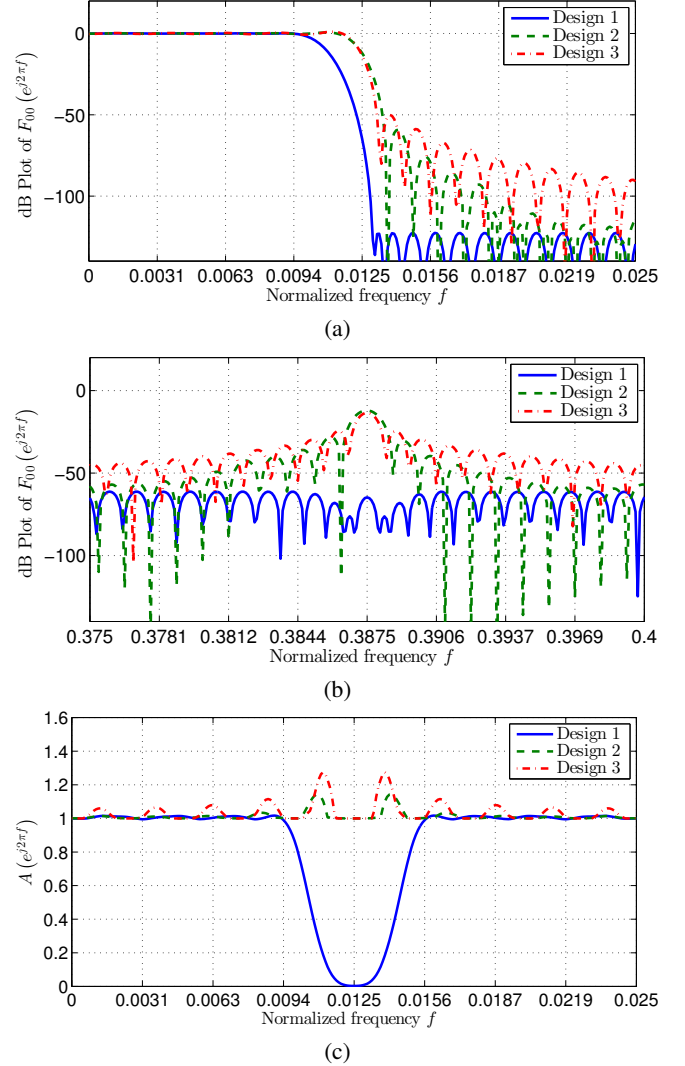

Fig. 2. A coprime DFTFB design example with $M = 6$, $N = 5$, $N_g = 100$, and $N_h = 120$. dB plots of $F_{00}\left(e^{j2\pi f}\right)$ showing (a) the passband behavior, (b) part of the stopband, and (c) overall amplitude responses.

6. CONCLUDING REMARKS

In this paper, we performed theoretical analysis on bumps in coprime DFTFBs and proposed an optimization problem that took the passband, the stopband, and the overall amplitude responses into consideration. Locations of bumps and tradeoffs between bumps and overall amplitude responses were explicitly established in Theorem 2 and Theorem 3. Also a new optimization problem regarding coprime DFTFB designs was formulated, approximated, and solved via alternating minimization. Our simulations showed this new approach gave us a better $A\left(e^{j2\pi f}\right)$.

In applications such as cognitive radio [14], good spectrum coverage is required. For coverage of the desired band, our new approach in this paper considers the overall amplitude responses and shows better performance than the designs in [7].

7. REFERENCES

[1] P. P. Vaidyanathan and P. Pal, "Sparse sensing with co-prime samplers and arrays," *IEEE Trans. Signal Process.*, vol. 59, no. 2, pp. 573–586, Feb 2011.

[2] P. Pal and P. P. Vaidyanathan, "Coprime sampling and the MUSIC algorithm," in *Proc. IEEE Digital Signal Processing Workshop and IEEE Signal Processing Education Workshop*, Jan 2011, pp. 289–294.

[3] P. P. Vaidyanathan and P. Pal, "Coprime sampling for system stabilization with FIR multirate controllers," in *Proc. IEEE Asil. Conf. on Sig., Sys., and Comp.*, 2011.

[4] J. Chen, Q. Liang, and B. Z. X. Wu, "Spectrum efficiency of nested sparse sampling and coprime sampling," *EURASIP Journal on Wireless Communications and Networking*, vol. 2013, no. 47, 2013.

[5] A. T. Moffet, "Minimum-redundancy linear arrays," *IEEE Trans. Antennas Propag.*, vol. 16, no. 2, pp. 172–175, 1968.

[6] K. Adhikari, J. R. Buck, and K. E. Wage, "Beamforming with extended coprime sensor arrays," in *Proc. IEEE Int. Conf. Acoust., Speech, and Sig. Proc.*, 2013, pp. 4183–4186.

[7] C.-L. Liu and P. P. Vaidyanathan, "Design of coprime DFT arrays and filter banks," in *Proc. IEEE Asil. Conf. on Sig., Sys., and Comp.*, 2014.

[8] Y. Neuvo, C.-Y. Dong, and S. K. Mitra, "Interpolated finite impulse response filters," *IEEE Trans. Acoust., Speech, Signal Process.*, vol. 32, no. 3, pp. 563–570, Jun 1984.

[9] T. Saramäki, Y. Neuvo, and S. K. Mitra, "Design of computationally efficient interpolated FIR filters," *IEEE Trans. Circuits Syst.*, vol. 35, no. 1, pp. 70–88, Jan 1988.

[10] P. P. Vaidyanathan, *Multirate Systems And Filter Banks*, Pearson Prentice Hall, 1993.

[11] T. Nagell, *Introduction to Number Theory*, New York: Wiley, 1951.

[12] T. F. Chan and C. K. Wong, "Convergence of the alternating minimization algorithm for blind deconvolution," *Linear Algebra and its Applications*, vol. 316, pp. 259–285, 2000.

[13] Y. Wang, J. Yang, W. Yin, and Y. Zhang, "A New Alternating Minimization Algorithm for Total Variation Image Reconstruction," *SIAM J. Imaging Sci.*, vol. 1, no. 3, pp. 248–272, 2008.

[14] B. Farhang-Boroujeny, "Filter bank spectrum sensing for cognitive radios," *IEEE Trans. Signal Process.*, vol. 56, no. 5, pp. 1801–1811, May 2008.